Responses of surface ozone to future agricultural ammonia emissions and subsequent nitrogen deposition through terrestrial ecosystem changes

Xueying Liu[1][*], Amos P. K. Tai[1,2,3], Ka Ming Fung[1][#]

[1]Earth System Science Programme and Graduate Division of Earth and Atmospheric Sciences, Faculty of Science, The Chinese University of Hong Kong, Sha Tin, Hong Kong SAR, China
[2]Institute of Environment, Energy and Sustainability, and State Key Laboratory of Agrobiotechnology, The Chinese University of Hong Kong, Sha Tin, Hong Kong SAR, China
[3]Center for Soybean Research of the State Key Laboratory of Agrobiotechnology, The Chinese University of Hong Kong, Hong Kong SAR, China
[*]Now at: Department of Earth and Atmospheric Sciences, University of Houston, Houston, TX, USA
[#]Now at: Department of Civil and Environmental Engineering, Massachusetts Institute of Technology, Cambridge, MA, USA

Correspondence to: Amos P. K. Tai (amostai@cuhk.edu.hk)

Abstract. With the rising food demands from the future world population, more intense agricultural activities are expected to cause substantial perturbations to the global nitrogen cycle, aggravating surface air pollution and imposing stress on terrestrial ecosystems. Much less studied, however, is how the terrestrial ecosystem changes induced by agricultural nitrogen deposition may modify biosphere-atmosphere exchange and further exert secondary feedback effects on global air quality. Here we examined the responses of surface ozone air quality to terrestrial ecosystem changes caused by 2000-to-2050 changes in agricultural ammonia emission and the subsequent nitrogen deposition by asynchronously coupling between the land and atmosphere components within the Community Earth System Model framework. We found that global gross primary production is enhanced by 2.1 Pg C yr^{-1} following a 20% (20 Tg N yr^{-1}) increase in global nitrogen deposition by the end of year 2050 in response to rising agricultural ammonia emissions. Leaf area index was simulated to be higher by up to 0.3–0.4 m^2 m^{-2} over most tropical grasslands and croplands, and 0.1–0.2 m^2 m^{-2} across boreal and temperate forests at midlatitudes. Around 0.1-0.4 m increases in canopy height were found in boreal and temperate forests, and ~0.1 m increases in tropical grasslands and croplands. We found that these vegetation changes could lead to surface ozone changes by ~0.5 ppbv when prescribed meteorology was used (i.e., large-scale meteorological responses to terrestrial changes were not allowed), while surface ozone could typically be modified by 2–3 ppbv when meteorology was dynamically simulated in response to vegetation changes. Rising soil NO_x emission from 7.9 to 8.7 Tg N yr^{-1} could enhance surface ozone by 2–3 ppbv with both prescribed and dynamic meteorology. We thus conclude that following enhanced nitrogen deposition, the modification of the meteorological environment induced by vegetation changes and soil biogeochemical changes are the more important pathways that can modulate future ozone pollution, representing a novel linkage between agricultural activities and ozone air quality.

1 Introduction

Increased food production for the ever-growing world population has been enabled by the widespread agricultural expansion and intensification with heavy fertilizer applications, which have correspondingly led to an enhancement in ammonia (NH_3) emission from the land by a factor of two to five since preindustrial times (Behera et al., 2013; Gu et al., 2015; Zhu et al., 2015). For instance, Asia (excluding Siberia), home to more than 60% of the world population (FAOSTAT, 2016), has experienced rapid expansion of agricultural activities (Liu & Tian, 2010; Tian et al., 2014), accounting for ~50% of the global total consumption of synthetic fertilizer and 30–40% of global manure production (FAOSTAT, 2016). Agriculture-related activities are known to be the most significant sources of atmospheric NH_3, of which the vast majority (~60%) originates from

the excessive use of nitrogenous fertilizer and concentrated operations of livestock feeding on a global scale (Huang et al., 2012; Paulot et al., 2014; Zhang et al., 2018); for Asia the percentage is even higher (80–90%) (Streets et al., 2003; Reis et al., 2009; Gu et al., 2012; Kang et al., 2016; Zhang et al., 2017; Zhang et al., 2018). Crops typically take up only about 40–60% of the nitrogen fertilizer applied to croplands (Tilman et al., 2002; Zhang et al., 2015; Liu et al., 2016; Muller et al., 2017), and only 25–35% of the nitrogen fed to dairy cows is converted into milk (Bittman et al., 2009), while most of the remainder is chemically transformed into a variety of simple and complex forms and leaked to the environment. The release of gaseous NH_3 into the atmosphere is one of the major nitrogen leakages from agricultural soils. Under a business-as-usual scenario where future nitrogen use efficiency (NUE; i.e., the fraction of nitrogen input finally harvested as output) in agricultural systems is not expected to be substantially improved, increasing food production will undoubtedly continue to intensify agricultural NH_3 emission into the overlying air (Erisman et al., 2008; Lamarque et al., 2011; Zhang et al., 2017).

Reactive nitrogen, from emissions of nitrogen oxides (NO_x; $NO+NO_2$) and NH_3, is deposited over land and ocean through a variety of processes collectively known as wet and dry deposition. As combustion-driven NO_x emission is projected to slow down due to regulatory efforts (van Vuuren et al., 2011) while agricultural NH_3 emission will continue to increase (Lamarque et al., 2011), future nitrogen deposition is expected to increase overall in the global budget (Galloway et al., 2004; Paulot et al., 2013; Lamarque et al., 2013; Kanakidou et al., 2016) and shift from a nitrate-dominated to ammonium-dominated condition (Ellis et al., 2013; Paulot et al., 2013; Li et al., 2016). Atmospheric nitrogen deposition onto the land surface is an important source of soil mineral nitrogen and thus enhances plants growth; this is known as the "nitrogen fertilization effect" (Reay et al., 2008; Templer et al., 2012). The fertilization effect depends on the soil "nitrogen limitation" defined as the nitrogen constraint on the productivity of many terrestrial ecosystems (Vitousek et al., 2002; Gruber and Galloway, 2008; LeBauer et al., 2008; Heimann et al., 2008; Reay et al., 2008; Zaehle et al., 2010). Nitrogen limitation is often found in natural soils where severe nitrogen competition among plants and microbes exists, and the unmet plant nitrogen demand can be translated to a reduction in the potential gross primary production (GPP) of the terrestrial ecosystems, representing a direct downregulation of photosynthetic carbon gain.

Nitrogen deposition affects the terrestrial carbon and nitrogen cycle, but much less is known about how nitrogen deposition affects atmospheric chemistry via terrestrial changes and feedbacks. As nitrogen limitation is relaxed, enhanced carbon assimilation can be translated to changes in the carbon mass allocated to different plant parts, ultimately manifested as an enhancement in vegetation structural variables such as leaf area index (LAI) and canopy height. Meanwhile, nitrogen deposition can also alter soil inorganic nitrogen composition and a variety of abiotic and biotic processes including uptake by plants, nitrification, denitrification, immobilization by microbes, and fixation in clay minerals. Soil NO_x is produced as a by-product of nitrification and denitrification, two microbial processes that first convert NH_3 aerobically to nitrate (NO_3^-) and then NO_3^- to nitrous oxide (N_2O) or nitrogen gas (N_2) under anoxic conditions. As LAI, canopy height and soil NO_x are known to affect surface air quality, nitrogen deposition can potentially affect atmospheric chemistry through affecting vegetation structure and ecophysiology, as well as soil biogeochemistry.

Nitrogen-mediated changes in vegetation and soil can affect surface ozone air quality via various pathways (Fig. 1). Among them, "biogeochemical" effects are processes mediated via direct exchange (i.e., emissions or deposition) of relevant chemical species between the terrestrial biosphere (vegetation and soil microbes) and the atmosphere, while "biogeophysical" or "meteorological" effects are mediated through a modification of the overlying meteorological environment (i.e., temperature, humidity, turbulence structure, etc.), as defined in Sadiq et al. (2017), Zhou et al. (2018) and Wang et al. (2020). One possible biogeochemical pathway is that LAI enhancement could elevate surface ozone by increasing biogenic volatile organic compound (VOC) emissions in high-NO_x environments, but could also reduce ozone by increasing dry-depositional uptake

1 via leaf stomata (Zhao et al., 2017). Another possible biogeochemical effect is via the increase in canopy height, which further

2 enhances surface roughness length, turbulent mixing and thus higher aerodynamic conductance for land-atmosphere exchange

3 including ozone dry deposition (Bonan, 2016; Oleson et al. 2013). Another possible biogeochemical effect is that increased

4 inorganic nitrogen availability facilitates soil NO_x emission through nitrification and denitrification processes, which further

5 causes rapid NO and NO_2 cycling for ozone formation. Biogeophysical effects or meteorological effects are through

6 vegetation-induced changes in the surface energy balance (e.g., absorbed solar radiation, sensible and latent heat fluxes) and

7 subsequent changes in surface temperature, precipitation, humidity, circulation patterns, moisture convergence (Wang et al.,

8 2020). Higher temperature enhances ozone mainly through increased biogenic emissions and higher abundance of NO_x, while

9 lower humidity reduces the chemical loss rate of ozone (Jacob and Winner, 2009; Fiore et al., 2012). Surface ozone changes

10 via each individual process are heterogeneous over the globe, and the overall ozone response through various biogeochemical

11 and biogeophysical pathways is highly complex (Zhao et al., 2017).

12
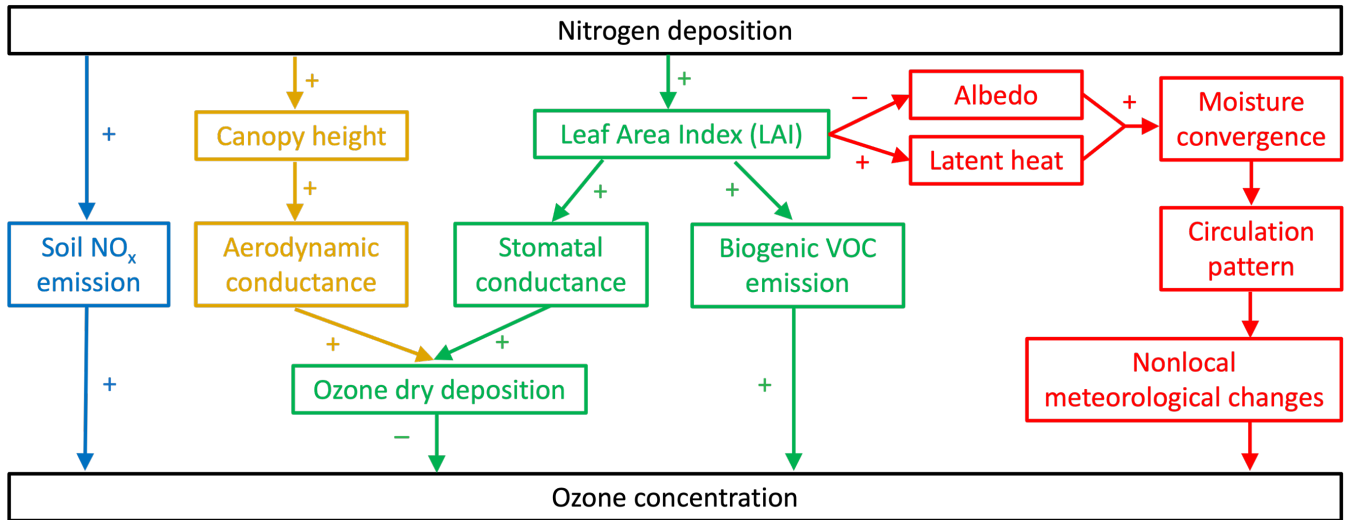
Figure 1. "Biogeochemical" and "biogeophysical" pathways of nitrogen deposition affecting surface ozone concentration.
Biogeochemical pathways via canopy height (yellow-colored), leaf area index (LAI; green-colored), and soil NO_x (blue-
colored), as well as some of the biogeophysical pathways relevant for this study (red-colored) are shown. The sign associated
with each arrow indicates the correlation between the two variables; the sign of the overall effect (positive or negative) of a
given pathway is the product of all the signs along the pathway. "Biogeochemical" pathways affect gas exchange (i.e. biogenic
VOC emission and ozone deposition) though plant stomata or microbe-mediated soil processes. "Biogeophysical" or
"meteorological" pathways are mediated through a modification of the local and nonlocal overlying meteorological
environment above the surface layer.

21

22 Here we present a study that investigates how agriculture-induced increases in NH_3 emission and subsequent nitrogen

23 deposition could affect surface ozone air quality via terrestrial ecosystem changes in terms of LAI, canopy height and soil NO_x

24 emission. We used an asynchronously coupled modeling framework based on the atmosphere (CAM-Chem) and land (CLM)

25 components of the Community Earth System Model (CESM) to quantify the corresponding responses of surface ozone air

26 quality to terrestrial changes. We first examined the responses of vegetation and soil variables to the present-day vs. future

27 scenarios of nitrogen deposition and then use those terrestrial changes to drive factorial simulations for surface ozone. To

28 evaluate the relative importance of LAI, canopy height and soil NO_x emission, we evaluated ozone responses to the three

29 individual effects and the overall combined effects using prescribed meteorology (i.e., large-scale meteorological responses to

30 terrestrial changes are not allowed). Furthermore, we evaluated the effects of changing meteorology to surface ozone by

31 conducting simulations using dynamic meteorology (i.e., where overlying boundary-layer meteorology and large-scale

32 circulation also responds to terrestrial changes). Model configuration with dynamic meteorology represents the overall effects

from regional terrestrial changes and associated meteorological changes (an integration over both biogeochemical and biogeophysical effects to surface ozone), whereas the setting with prescribed meteorology provides limited above-surface layer meteorological changes directly caused by terrestrial changes and represents the biogeochemical effects only. Our study emphasizes the complexity of biosphere-atmosphere interactions and their indirect modulating effects on air quality and atmospheric chemistry, which are important for evaluating the impacts from future food production trends on air quality and health beyond the direct effects of agricultural emissions alone.

2 Model and Method

2.1 Model description

We used the Community Earth System Model (CESM), which includes atmospheric, land, ocean and sea ice model components. We employed CESM version 1.2.2 with fully interactive atmosphere and land components, but with prescribed ocean and sea ice consistent. For the atmosphere component, we used the Community Atmosphere Model version 4 (CAM4) (Neale et al., 2010) fully coupled with an atmospheric chemistry scheme (i.e., CAM-Chem) that contains full tropospheric O_3-NO_x-CO-VOC-aerosol chemistry based on the MOZART-4 mechanism (Emmons et al., 2010; Lamarque et al., 2012). Emissions are from the combined emission inventories of the Emissions Database for Global Atmospheric Research (EDGAR), Regional Emission inventory in ASia (REAS) and Global Fire Emissions Database (GFED2) and others. CAM-Chem provides the flexibility of performing climate simulations online (i.e., "dynamic meteorology") and simulations with specified meteorological fields (i.e., "prescribed meteorology"). For simulations with dynamic meteorology, it was driven by the Climatic Research Unit – National Centers for Environmental Prediction (CRU-NCEP) climate forcing dataset. For simulations with prescribed meteorology, year-2000 and 2001 horizontal wind components, air temperature, surface temperature, surface pressure, sensible and latent heat flux and wind stress of the Goddard Earth Observing System Model version 5 (GEOS-5) forcing data at six hour interval were used (see Table 1). This version of CAM-Chem simulates the concentrations of 56 atmospheric chemical species at a horizontal latitude-by-longitude resolution of 1.9°×2.5° and a vertical resolution of 26 layers for dynamic meteorology and 52 layers for prescribed meteorology.

For the land component, we used the Community Land Model version 4.5 (CLM4.5) (Oleson et al., 2013) with Satellite Phenology (CLM45SP) mode where vegetation structures are prescribed (e.g., using satellite-derived LAI data), or with active carbon–nitrogen biogeochemistry (CLM45BGC) that contains prognostic treatment of terrestrial carbon and nitrogen cycles (Lawrence et al., 2011), depending on the cases of concern. In CLM4.5, the Model of Emissions of Gases and Aerosols from Nature (MEGAN) version 2.1 was used to compute biogenic emissions online as functions of LAI, vegetation temperature, solar radiation, soil moisture and other environmental conditions (Guenther et al., 2012). For dry deposition of gases and aerosols we used the resistance-in-series scheme in CLM4.5 as described in Lamarque et al. (2012) with updated, optimized coupling of stomatal resistance to LAI (Val Martin et al., 2014). Soil NO_x emission was implemented by Fung et al. (2021) as a function of N_2O emission, soil air-filled pore space and volumetric soil water content during nitrification and denitrification (See Supplementary for details). We also applied a temperature factor to correct the soil NO_x overestimation at high latitudes as previous studies (Zhao et al., 2017). Evapotranspiration rate was calculated based on the Monin-Obukhov similarity theory for turbulent exchange and the diffusive flux-resistance model with dependence on vegetation, ground and surface temperature, specific humidity, and an ensemble of resistances that are functions of meteorological and land surface conditions (Oleson et al., 2013; Lawrence et al., 2011; Bonan et al., 2011).

2.2 Asynchronously coupled atmosphere chemistry-biosphere modeling framework

An asynchronously coupled system with CAM-Chem and CLM was adopted to investigate the vegetation structural changes induced by nitrogen deposition and their potential to modulate surface ozone under both dynamic and prescribed meteorology. Asynchronous instead of synchronous coupling was used because currently CESM does not have the capacity to allow "online" bidirectional exchange of reactive nitrogen fluxes between the atmosphere and land components; it also conveniently facilitates sensitivity experiments to be conducted to isolate individual drivers of changes and processes. First, present-day and future scenarios of nitrogen deposition are obtained by CAM-Chem simulations with the corresponding NH_3 emission of year 2000 and 2050. Year-2000 NH_3 emission was from the prescribed emission inventory inherent in CAM-Chem (see Sect. 2.1), which includes anthropogenic, ocean, soil and biomass burning sources. We split the year-2000 anthropogenic NH_3 emission into agricultural and non-agricultural parts by using the corresponding ratios based on the Magnitude And Seasonality of Agricultural Emissions model for NH_3 (MASAGE_NH3) (Paulot et al., 2014). We kept natural and non-agricultural emissions the same in both the year-2000 and year-2050 scenarios, and only scaled the year-2000 agricultural NH_3 by a growth factor g (Fig. 2c)

$$g = \frac{\text{crop production in 2050}}{\text{crop production in 2000}} \qquad\qquad\qquad \text{Eq.1}$$

based on crop production estimates from Alexandratos and Bruinsma (2012) accounting for technology-driven yield improvements and cropland area changes, as in Tai et al. (2014; 2017). We generated the growth factors for major crops (Fig. S1) and obtained an average growth factor from these crop-specific production growths. Such a linear scaling assumes nitrogen-use efficiency (NUE) of fertilization applications to remain the same in the future. In practice NUE is expected to rise with technological advancements, the extent of which is however highly uncertain and region-specific; we therefore regarded our linear scaling as a representation of the "worst-case" scenario where fertilizer nitrogen use remains as inefficient as it is today. For each scenario of the sensitivity experiments, CAM-Chem simulations were conducted for 20 simulation years. Throughout the CAM-Chem component was still coupled online with CLM45SP with prescribed vegetation structures, which computed land-atmosphere fluxes for CAM-Chem to simulate atmospheric dynamics and chemistry. Both simulations were performed with prescribed sea surface temperature and sea-ice cover following the HadISST dataset (Rayner et al., 2003) at the year-2000 level. Long-lived greenhouse gases and their radiative forcing were kept at year-2000 level to exclude the effects of increasing temperature on NH_3 emissions. The first five years of outputs were treated as spin-up and thus discarded in the analysis, and we calculated the annual averages of the last 15 years to obtain the corresponding nitrogen deposition fluxes for the year-2000 and year-2050 scenarios.

The CLM45BGC mode was used to investigate vegetation and soil changes in response to perturbations in the nitrogen input to the land. We first obtained steady-state vegetation and soil variables including LAI, canopy height and soil NO_x emission following present-day nitrogen deposition (obtained above CAM-Chem) for 200 years in CLM. The first 150 years of outputs were treated as spin-up, while the last 50-year average was used to represent the vegetation and soil conditions in a steady state. We used the year-2000 steady state as initial conditions for the following perturbation experiments. We then perturbed the present-day steady state with future nitrogen deposition fluxes following the year-2050 agricultural emission scenario, allowing the vegetation and soil variables to come into a "new" steady state, which took 10–20 simulations years. After that, the simulation was conducted for another 50 years, which were considered to be year-2050 steady state and then averaged to determine the differences in LAI, canopy height and soil NO_x emission from the 50-year present-day averages.

Last, we investigated the individual and combined impacts of the above changes in the three terrestrial pathways (i.e., via LAI, canopy height and soil NO_x emission) on surface ozone air quality, with both prescribed meteorology (i.e., large-scale meteorological responses to terrestrial changes are not allowed) and dynamic meteorology (i.e., overlying boundary-layer

1   meteorology and large-scale circulation also responds to terrestrial changes). Terrestrial changes with prescribed meteorology

2   included only biogeochemical pathways, while terrestrial changes with dynamic meteorology included the combined effects

3   of biogeochemical and biogeophysical processes as well as larger meteorological and circulation pattern changes. Therefore,

4   we were able to examine the effects from land-atmosphere feedbacks with dynamic meteorology, while prescribed

5   meteorology provided limited atmospheric changes directly caused by terrestrial changes without much land-atmosphere

6   feedbacks. To evaluate the relative importance of individual pathways to the overall effects, we conducted four sets of fully

7   coupled land-atmosphere simulations: (1) a control case without any nitrogen-mediated changes in LAI, canopy height and

8   soil NO_x emission ([CTR]); (2) a simulation with LAI change only ([LAI]); (3) a simulation with canopy height change only

9   ([HTOP]); (4) a simulation with soil NO_x emission change only ([NOX]); (5) a simulation with all changes in LAI, canopy

10   height and soil NO_x emission ([ALL]). Simulation [LAI], [HTOP] and [NOX] in relation to [CTR] allowed us to quantify the

11   relative contribution from LAI, canopy height and soil NO_x emission respectively, while simulation [ALL] reflected the overall

12   ozone changes due to three combined effects. The experiments were summarized in Table 1. We conducted the same set of

13   simulations with both dynamic and prescribed meteorology to examine how meteorological responses to these terrestrial

14   changes would modify the importance of these pathways (Table 2). We focused on average changes in the last 15-year northern

15   summer (June, July and August: JJA) for most of the variables in the rest of this paper, since summer was both the high-ozone

16   season and the growing season of the majority of global vegetation, when ozone-vegetation coupling appeared to be the

17   strongest and significant.

18

19   **Table 1.** Meteorological inputs for simulations with dynamic and prescribed meteorology.

	Dynamic	Prescribed
Meteorology	Simulated within CAM	GEOS-5 reanalysis data
Terrestrial changes	[CTR], [LAI], [HTOP], [NOX], [ALL]	[CTR], [LAI], [HTOP], [NOX], [ALL]

20

21   **Table 2.** Experimental design to quantify surface ozone responses to terrestrial changes including leaf area index (LAI), canopy

22   height, and soil NO_x emission.

	[CTR]	[LAI]	[HTOP]	[NOX]	[ALL]
LAI	Year 2000	Year 2050	Year 2000	Year 2000	Year 2050
Canopy height	Year 2000	Year 2000	Year 2050	Year 2000	Year 2050
Soil NO_x	Year 2000	Year 2000	Year 2000	Year 2050	Year 2050

23

24   **3 Year-2000 vs. year-2050 NH_3 emissions and nitrogen deposition**

25   We first show the year-2000 emissions of reactive nitrogen as NO_x (48 Tg N yr^{-1}, Fig. 2a) and NH_3 (53 Tg N yr^{-1}, Fig. 2b),

26   with a global budget of 101 Tg N yr^{-1}, in good agreement with Ciais et al. (2013). NO_x is densely emitted from industrial and

27   populated regions, while hotspots for NH_3 emission are India and eastern China with intensive agricultural activities and

28   inefficient fertilizer use. Global year-2050 NH_3 emission is projected to reach 67, 57, 65 and 71 Tg N yr^{-1} in Representative

29   Concentration Pathway (RCP) RCP2.6, RCP4.5, RCP6.0 and RCP8.5 respectively, mainly due to rising agricultural production

30   (RCP database version 2.0.5). Yet RCP projections did not include a sufficient representation of the spatial patterns of

31   agricultural NH_3 emissions worldwide and especially in Asia, the world's most productive croplands (RCP database version

32   2.0.5). To capture 2000-to-2050 agricultural intensification, we therefore estimated future NH_3 emission based on FAO 2000-

33   to-2050 crop production changes.
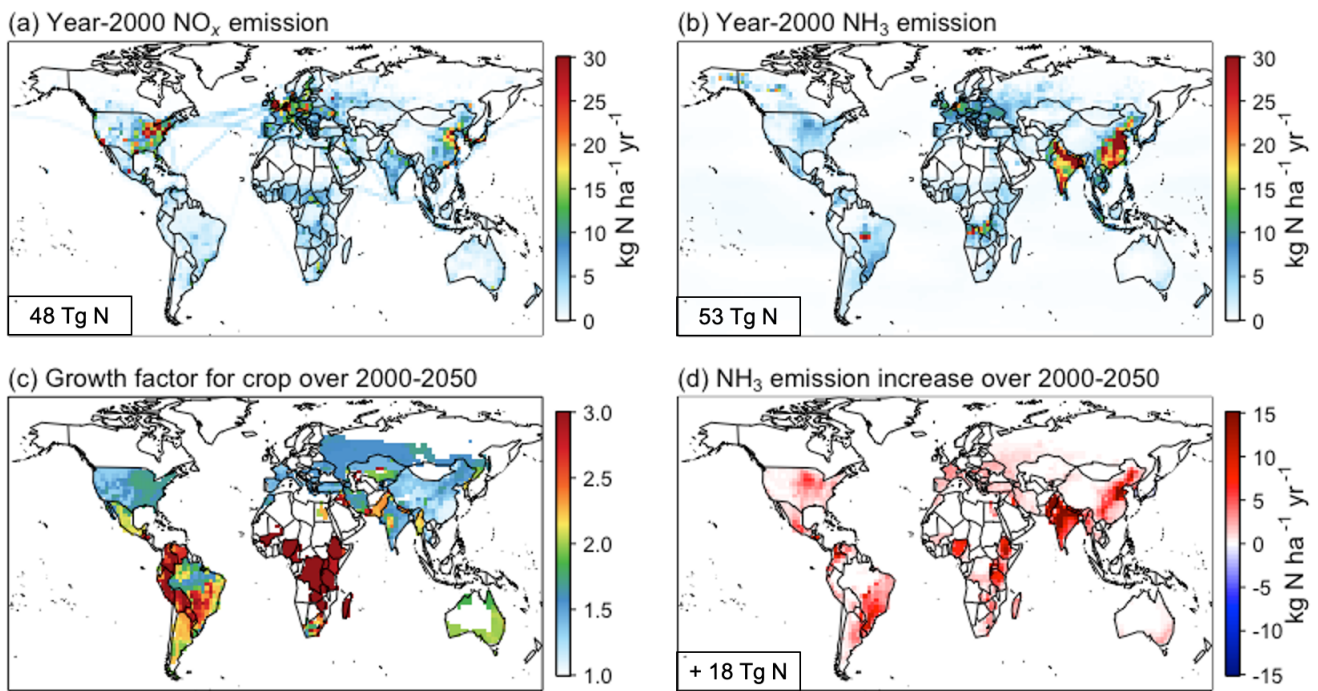
Figure 2. Global year-2000 emissions of **(a)** NO$_x$ and **(b)** NH$_3$, **(c)** growth factor g of crop production increase over 2000–2050 from the Food and Agriculture Organization of the United Nations (FAO), and **(d)** projected increases in NH$_3$ emission over 2000–2050.

FAO projects global year-2050 crop production to be higher than year-2000 level due to changes in yield, crop intensity (i.e., multiple cropping, shortening of fallow periods), and arable land (Alexandratos and Bruinsma, 2012). The major increases occur in South America and Central Africa due to yield increases and arable land expansion. Production growth factor g in Fig. 2c can go up to 2–3 for South America and 3–5 for Central Africa, while it is 1.5–2 for some of the world's most productive croplands at northern midlatitudes, suggesting that the Southern Hemisphere will be playing an increasingly important role in producing food for the future global population. By scaling up year-2000 NH$_3$ emission by growth factor in FAO crop production, we estimated that year-2050 NH$_3$ budget to be 71 Tg N yr^{-1}, a 34% increase (18 Tg N yr^{-1}) compared to year-2000 emission, with major increases over East China, India, Midwestern United States, Brazil, Argentina and East Africa (Fig. 2d). This estimate is comparable to the RCP8.5 estimate of 71 Tg N yr^{-1} as both studies assumed a business-as-usual scenario where future NUE in agroecosystems is not expected to be improved much. We fed both year-2000 and year-2050 NH$_3$ emissions into the CESM model to simulate the corresponding nitrogen deposition. Global budget of both reduced (NH$_x$) and oxidized (NO$_y$) nitrogen deposition is 101 Tg N yr^{-1} in year 2000 (Fig. 3a), which almost balances out the emission totals of both NH$_3$ and NO$_x$. Nitrogen deposition in 2050 is 121 Tg N yr^{-1}, a 20% (20 Tg N yr^{-1}) increase from the year-2000 total (Fig. 3b). Increases in 2000-to-2050 nitrogen deposition mostly result from increased NH$_x$ deposition, since we fixed the NO$_x$ emission at year-2000 level to isolate the deposition changes due to agricultural intensification alone. These increased nitrogen deposition serves as an important input of mineral nitrogen from the atmosphere to the biosphere.
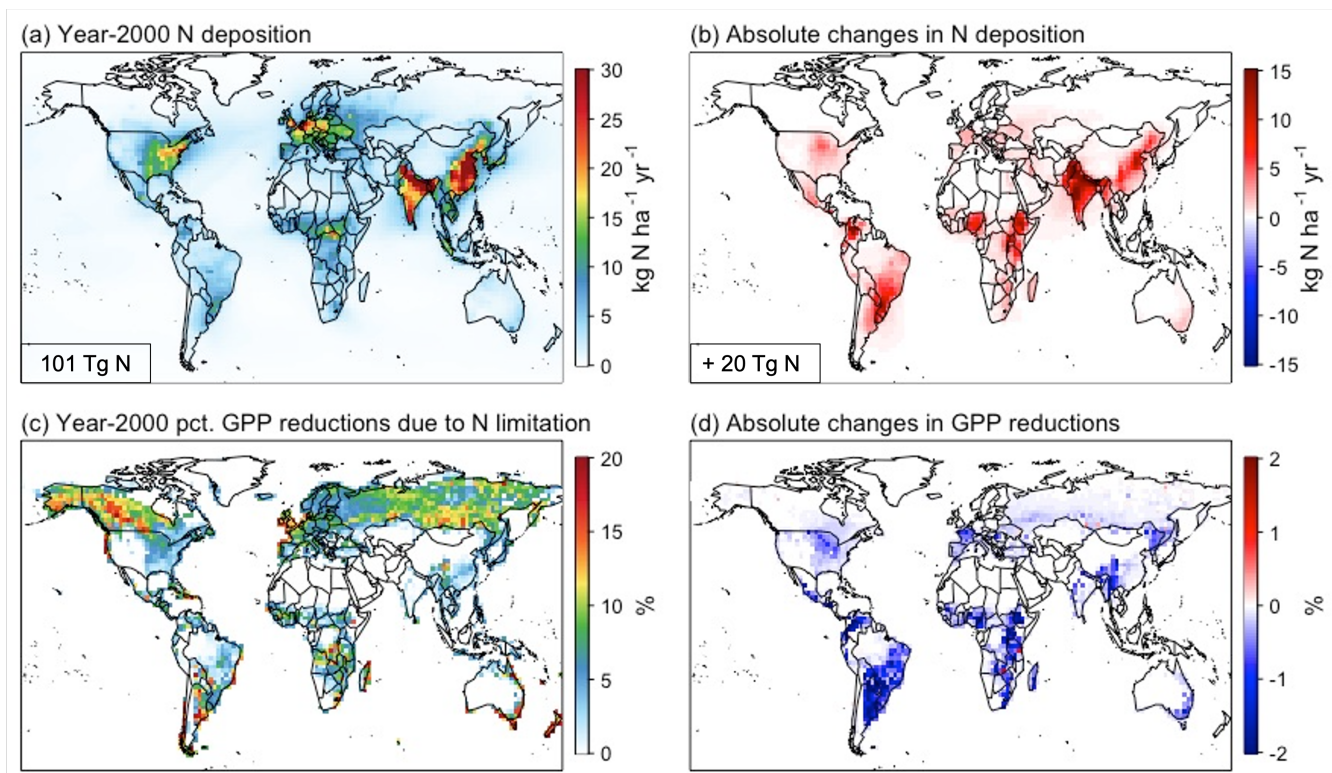
Figure 3. (a) Year-2000 atmospheric nitrogen deposition and **(b)** absolute changes in nitrogen deposition over 2000–2050. **(c)** Year-2000 gross primary production (GPP) percentage reduction due to nitrogen limitation as presented in the CLM model. In nitrogen-limited soils (i.e., colored areas), plant growth is limited by insufficient soil nitrogen supply due to plant-microbe competition. **(d)** Absolute changes in nitrogen limitation-induced GPP reductions because of enhanced nitrogen availability from atmospheric nitrogen deposition over 2000–2050. Relative changes over 2000–2050 can be found in supplementary Figure S2.

4 Responses of terrestrial ecosystems to nitrogen deposition

We present in this section the fertilization effect of year-2050 nitrogen deposition and associated enhancements in vegetation structure (i.e., LAI and canopy height) and soil NO_x emission compared with those of year-2000 nitrogen deposition. Nitrogen uptake from the soil is an important determinant of plant growth, as nitrogen is a major component of chlorophyll (i.e., pigments absorbing light energy for photosynthesis) and Rubisco (i.e., enzyme necessary for carbon fixation). Meanwhile, mineral nitrogen availability is also vital for nitrification and denitrification microbial processes where NO_x is produced as a by-product. In CLM, the plant nitrogen demand for new growth is calculated by the carbon available for allocation to new growth allocation, given the C:N stoichiometry of a given plant type and plant part. From the soil side, soil mineral nitrogen supply is calculated by adding various nitrogen sources (e.g., atmospheric nitrogen deposition, fertilizer, biological nitrogen fixation) and subtracting nitrogen sinks (e.g., leaching, assimilation by heterotrophs). When the plant nitrogen demand is greater than the soil nitrogen supply, the plants are not able to take up enough nitrogen to support the carbon allocation for new growth, which would then be reduced ("downregulated") by a percentage in the model, which we refer as soil "nitrogen limitation" on plant growth here. When the soil is "nitrogen-limited", the plants are not able to take up enough nitrogen for maximum photosynthesis and unmet plant nitrogen demand is translated back to a carbon supply surplus which is eliminated through reduction of GPP in the CLM model. Figure 3c shows the year-2000 GPP percentage reductions due to nitrogen limitation. Most of the nitrogen-limited soils are found over the boreal forests because of slow soil decomposition and turnover with litter of high C:N content and cold climate. Savannas and grasslands in the tropics are also mildly nitrogen-limited because of low foliar nitrogen concentrations and plant density. Figure 3d shows the differences of GPP reductions, i.e., year-2050

8

GPP reductions minus year-2000 GPP reductions. We found smaller GPP reductions induced by nitrogen limitation in 2050 than 2000, reflecting higher plant productivity and growth over 2000–2050. However, this nitrogen fertilization effect is found only over nitrogen-limited regions, but not over nitrogen-abundant regions such as India and northern China where the critical nitrogen loads are almost always exceeded (Zhao et al., 2017) despite of substantial increases of nitrogen deposition over 2000–2050.

Due to nitrogen fertilization, GPP, LAI, canopy height and soil NO_x emission over nitrogen-limited regions are generally higher with year-2050 nitrogen deposition (Fig. 4). Specifically, we found that year-2050 nitrogen deposition to the land enhances global GPP by 2.1 Pg C yr^{-1} (Fig. 4e), and the enhanced carbon assimilation can be translated into changes in the carbon mass allocated to different plant parts such as leaves, stems and roots. The two vegetation structural proxies in the CLM model, LAI and canopy height, which characterize the carbon allocation to plant tissues leaf and stem, respectively. LAI was simulated to be higher by up to 0.3–0.4 m^2 m^{-2} over tropical grasslands and croplands in Brazil, savannas in Sub-Saharan Africa, and 0.1–0.2 m^2 m^{-2} across boreal and temperate forests at midlatitudes (Fig. 4f). Canopy heights from broadleaf deciduous trees and needleleaf evergreen trees were simulated to be higher by up to 0.1–0.3 m over the eastern US, southern Europe, southern Russia and southeastern China, and increases of 0.3–0.4 m were found over broadleaf deciduous trees in South America, and ~0.1 m increases were found for grasses and crops over Sub-Saharan Africa (Fig. 4g). Meanwhile, global soil NO_x emission budget rises from 7.9 Tg N yr^{-1} to 8.7 Tg N yr^{-1} (Fig. 4h) due to faster and greater nitrification and denitrification processes under year-2050 atmospheric nitrogen deposition.
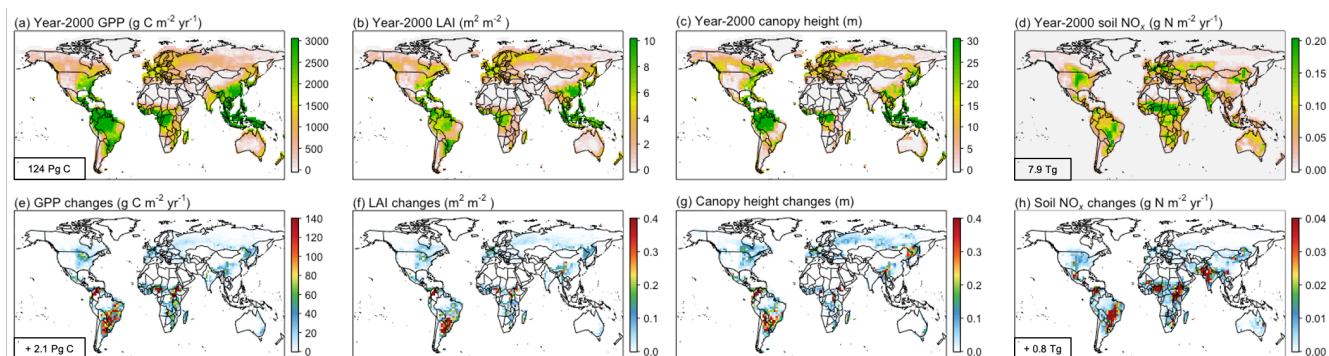
Figure 4. Annual mean of year-2000 **(a)** gross primary production (GPP), **(b)** leaf area index (LAI), **(c)** canopy height, **(d)** soil NO_x emission, and corresponding increases **(e-h)** due to increased nitrogen deposition over 2000–2050.

5 Impacts of terrestrial changes on surface ozone air quality

5.1 Surface ozone changes with prescribed meteorology

We first examined the responses of surface ozone air quality to changes in LAI, canopy height and soil NO_x separately, as well as the combined effects of all, with prescribed meteorology (i.e., large-scale meteorological responses to these terrestrial changes are not accounted for in the ozone changes). With prescribed meteorology, the responses of ozone are seen mostly where the changes in vegetation cover or soil emission take place. Figure 5d shows that LAI modulates surface ozone biogeochemically (i.e., without perturbing the overlying meteorology) by ±0.5 ppbv depending on the counteracting effects from enhanced biogenic VOC emission (Fig. 5e) and surface conductance for ozone deposition (Fig. 5d). We estimated a 3.0 Tg yr^{-1} increase in global biogenic isoprene emission (Fig. 5e), a key source of reduced atmospheric hydrocarbons that are the chief precursors of tropospheric ozone. Yet, rises in dry deposition velocity (Fig. 5f) reduce ozone concentration. The sensitivity of isoprene emission to LAI is higher than that of dry deposition, rendering the effects of isoprene emission

dominant in northern midlatitude regions with low LAI to begin with (Wong et al., 2018). As shown in Fig. 5g, increased canopy height decreases ozone by 0.2 ppbv through stronger aerodynamic conductance and thus stronger turbulent exchange and dry deposition within the surface layer (without the corresponding changes in the overlying boundary-layer meteorology, however, due to prescribed meteorology). Ozone dry deposition velocity increases by 0.002–0.004 cm s^{-1}, with increased canopy height in central Africa and the northern US. Figure 5j shows that surface ozone is elevated biogeochemically by 1–3 ppbv in certain low-NO$_x$ equatorial regions due to increased soil NO$_x$ emission. Overall ozone changes with prescribed meteorology (Fig. 5m) are mostly local and can be explained predominately (80–90%) by biogeochemical effects from soil NO$_x$ emission.
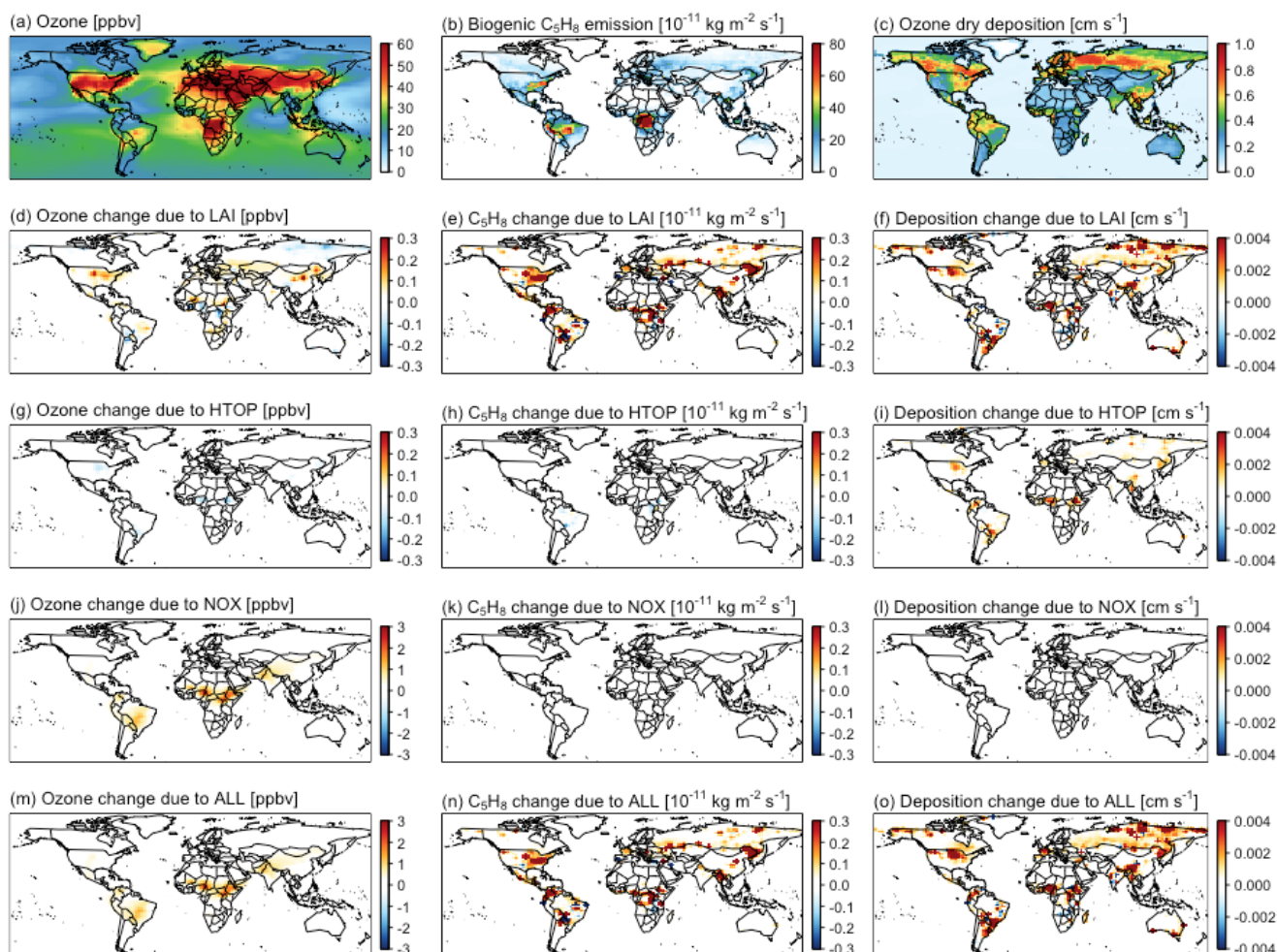

Figure 5. Year-2000 summertime (June-July-August; JJA) level of **(a)** surface ozone concentration, **(b)** biogenic isoprene emission, **(c)** ozone dry deposition, and their corresponding changes due to nitrogen-mediated increases in LAI only **(d, e, f)**, canopy height only **(g, h, i)** and soil NO$_x$ emission only **(j, k, l)**, and the combination increases of all **(m, n, o)** with prescribed meteorology.

5.2 Surface ozone changes with dynamic meteorology

To evaluate the relative importance of regional terrestrial changes vs. terrestrial changes with meteorological changes in regulating surface ozone concentration, we also conducted simulations with dynamic meteorology (i.e., overlying boundary-layer meteorology and large-scale circulation could respond to terrestrial changes). The ozone changes with dynamic meteorology are the combined results from regional terrestrial changes and associated meteorological changes, an integration over both biogeochemical and biogeophysical effects. Figure 6 shows that the changes in summertime surface ozone are within

±2–3 ppbv with dynamic meteorology. Overall ozone change with dynamic meteorology (Fig. 6m) are the combined results from the integrated effects of vegetation changes (Fig. 6d, g) as well as biogeochemical effects of soil NO_x changes (Fig. 6j).

Ozone changes in response to vegetation changes with dynamic meteorology (Fig. 6d, g) are much higher than those with prescribed meteorology (Fig. 5d, g) as vegetation changes could modify boundary-layer meteorology, shift circulation patterns and moisture flows, and thus shape ozone concentrations. In contrast to the clear, localized signals in ozone changes through the biogeochemical pathways, both local and remote surface ozone changes are found when biogeophysical pathways are involved (Wang et al., 2020). For example, changes in biogenic VOC emission with dynamic meteorology correlate with air temperature changes (Fig. S3, S4) apart from local vegetation changes. Changes in dry deposition also correlate to meteorological changes; stomatal resistance can respond to atmospheric dryness and soil water stress (Fig. S3, S4). Ozone changes in response to soil NO_x changes with dynamic meteorology (Fig. 6j) are within the same magnitude as those with prescribed meteorology (Fig. 5j), as soil NO_x emissions only change photochemical production of surface ozone, but do not affect biogenic VOC emission and ozone dry deposition directly (Fig.5 k, l) or via meteorological changes indirectly (Fig.6 k, l).
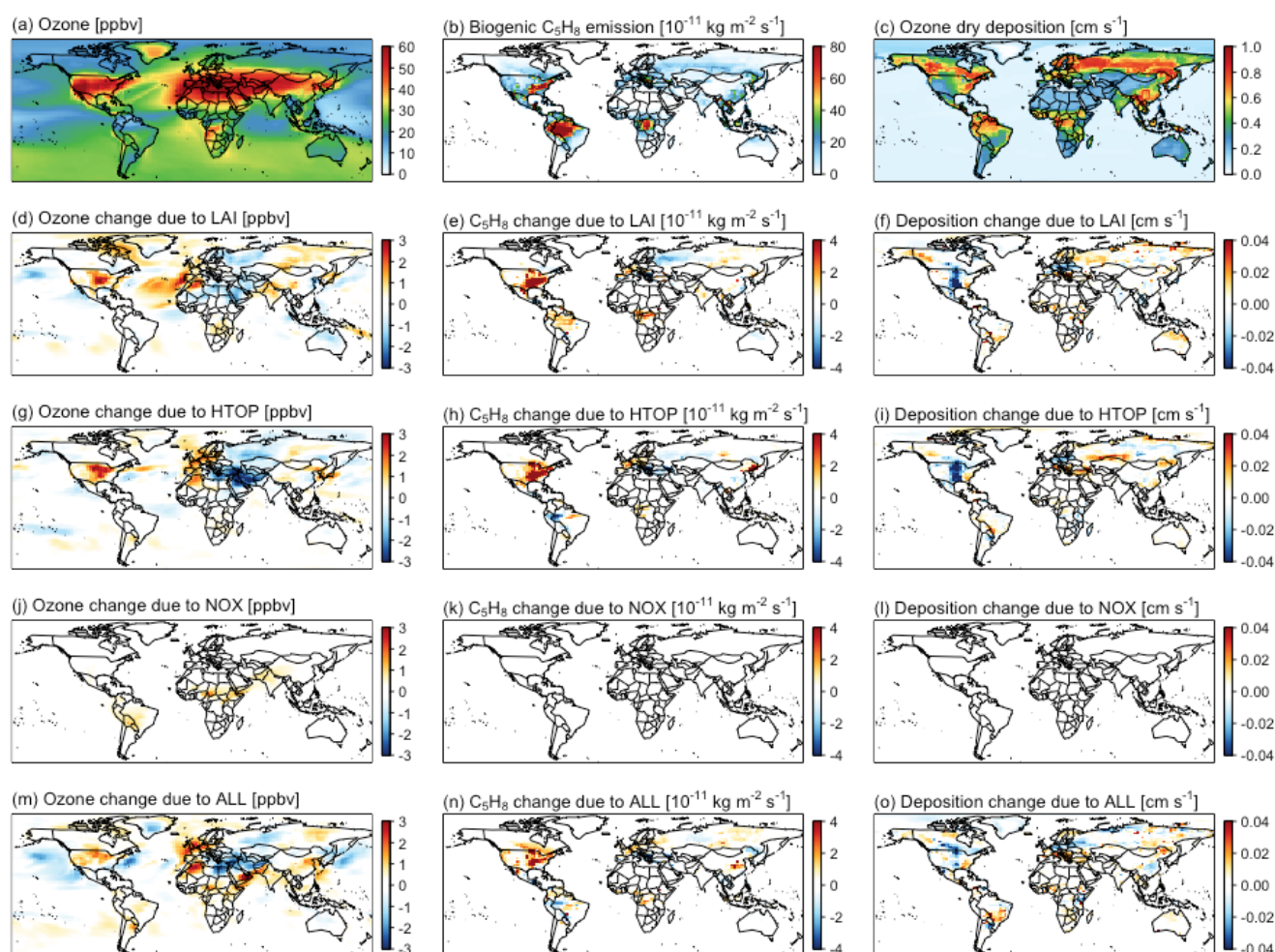

Figure 6. Same as Fig. 5 but with dynamic meteorology.

The greatest vegetation enhancements in response to future nitrogen deposition in this study are found over tropical savannas and grasslands, which are less capable of affecting local and pan-regional climate than forests, and our forest structural changes are only mild. Therefore, here we choose the US, which shows obvious ozone enhancement following vegetation changes, as an example to illustrate the biogeophysical effects further. Figure 7 shows that in the forest regions in the eastern US where

LAI and canopy height changes are relatively large following higher nitrogen deposition, albedo decreases, absorbed radiation increases, latent heat flux increases, and such changes appear to have shifted the surface energy balance and circulation patterns in a way that enhances moisture convergence, precipitation and soil moisture in the originally wetter places (i.e., the forested eastern US), but reduces the moisture convergence in the originally drier places (i.e., the grassland regions in the central US). This constitutes a feedback loop in these grassland regions that reduces transpiration, increases temperature, increases aridity and thus the plant stomata close more, all leading to the relatively large enhancements in surface ozone there. Our mild vegetation changes only have modest local impacts in places with dense vegetation to begin with (e.g., the eastern US). We found that vegetation changes shift the circulation patterns and moisture convergence such that it is the adjacent places that are the most affected, which was also found by Wang et al. (2020), who found obvious temperature increases in the central US after reforestation in the eastern US under RCP4.5 land use and land cover change. High temperature and reduced stomatal conductance in the central US further cause reduced ozone deposition (Fig. 6f), while increased temperature and LAI in the eastern US enhances biogenic emissions, both of which increase surface ozone in the central-eastern US (Fig. 6d).
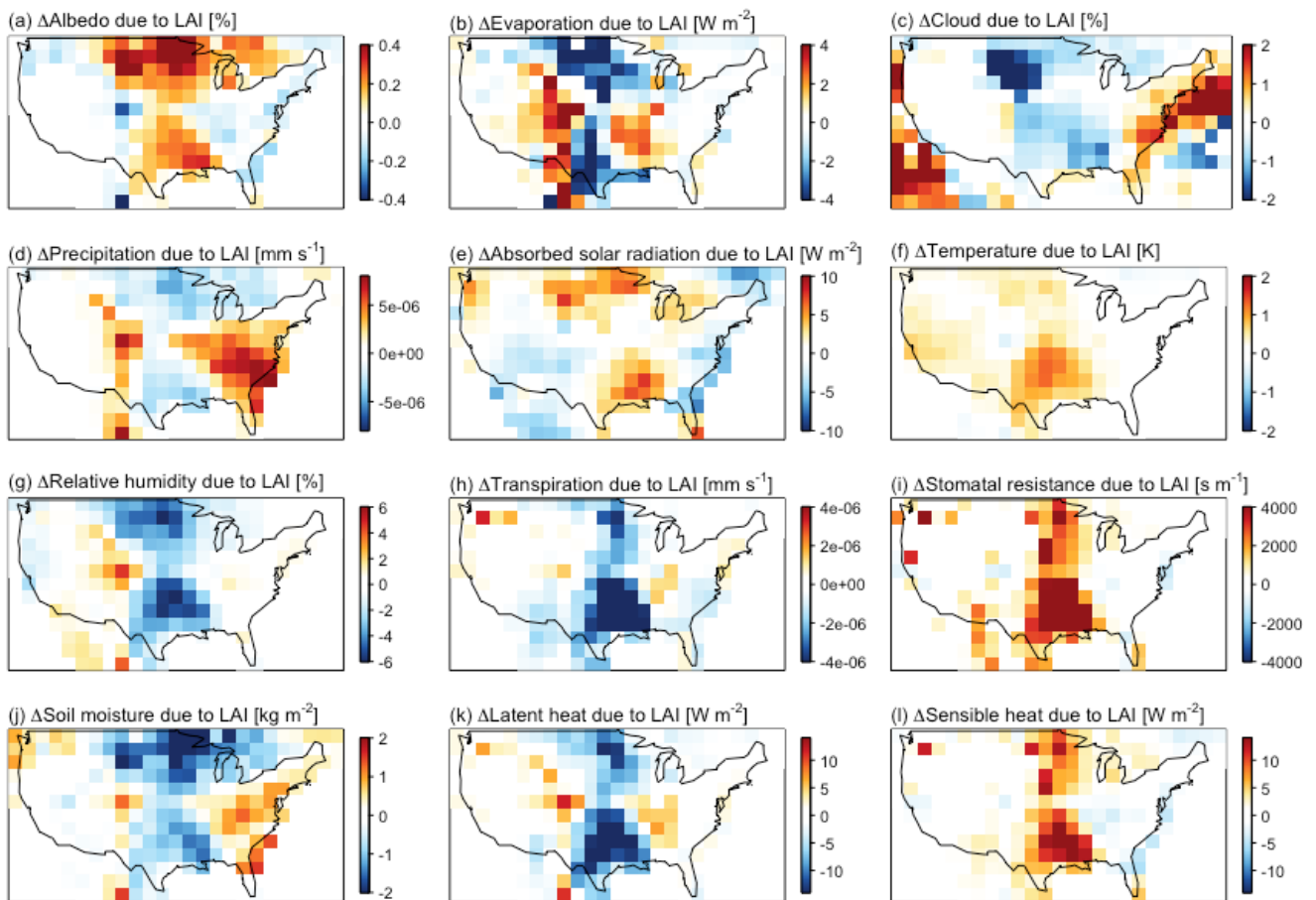
Figure 7. Summertime changes in **(a)** albedo, **(b)** ground evaporation, **(c)** cloud cover, **(d)** precipitation, **(e)** absorbed solar radiation, **(f)** surface temperature, **(g)** relative humidity, **(h)** vegetation transpiration, **(i)** stomatal resistance, **(j)** soil moisture, **(k)** latent heat flux, and **(l)** sensible heat flux driven by LAI increase with dynamic meteorology.
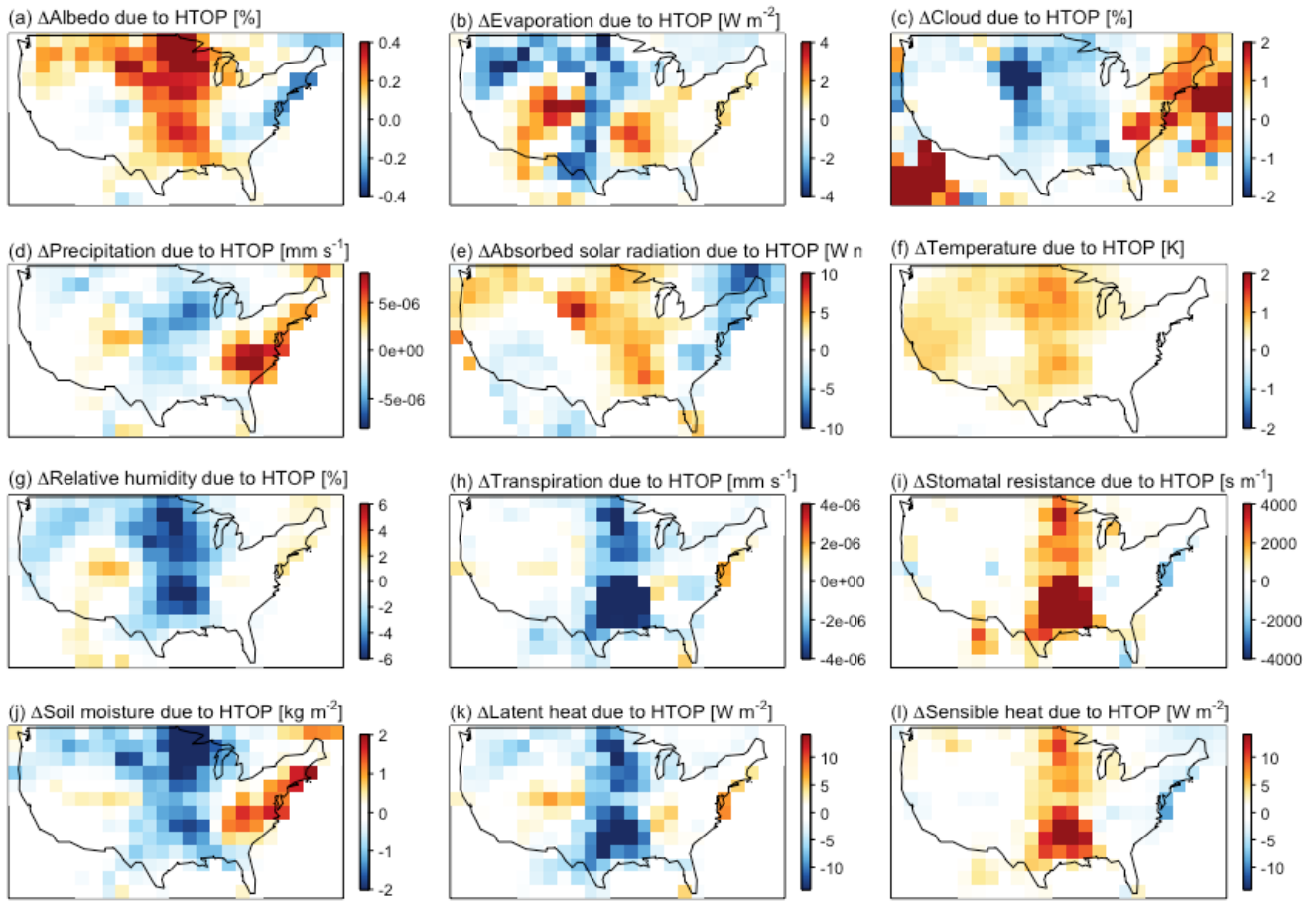
Figure 8. Same as Fig.7 but driven by canopy height increase.

Changes in canopy height show similar trends in modulating meteorological conditions (Fig. 8). The effects of meteorological variations induced by vegetation changes can be as important as or even more important than the direct biogeochemical effects of vegetation structural changes per se in terms of modulating surface ozone, and are of similar magnitude to the biogeochemical effects of soil NO_x changes. We note specifically that temperature changes resulted from vegetation-meteorology coupling are more important than LAI changes per se in regulating biogenic isoprene emission, especially in regions where obvious warming or cooling occurs. It is noteworthy that unlike with prescribed meteorology, individual effects may not add up linearly with dynamic meteorology for a given location due to the complex and far-reaching changes in atmospheric circulation and the associated cascade of local and nonlocal changes in climate that are dynamically simulated following terrestrial changes.

6 Conclusions

With the rising food need for the future world population, more intense agricultural activities are expected to cause substantial perturbations to the global nitrogen cycle, aggravating surface air pollution and imposing stress on terrestrial ecosystems. Much less studied, however, is how the ecosystem changes induced by agricultural nitrogen deposition may modify biosphere-atmosphere exchange and further exert secondary effects on global air quality. In this paper we present a study to quantify the response of surface ozone air quality to vegetation structural (LAI and canopy height) and soil NO_x emission changes under year-2000 vs. year-2050 agricultural ammonia emissions over centurial timescales by using an asynchronously coupled framework.

1 Agricultural ammonia emission in the coming decades is destined to increase. We estimated year-2050 NH_3 emission to be 71

2 Tg N yr^{-1}, a 34% increase compared to year-2000 emission. Our estimate is comparable to 71 Tg N yr^{-1} made by RCP8.5 as

3 both studies assumed a business-as-usual scenario where future NUE in agroecosystems is not expected to be improved much.

4 However, it should be acknowledged that increases in food production may also be obtained with a less-than-proportionate

5 increase in fertilizer use as countries are developing greater awareness of agriculture-related environmental impacts, and

6 adopting more efficient nutrient use practices in the coming decades. Gu et al. (2015) reported that reasonable changes in diet,

7 NUE, and N recycling could reduce year-2050 N losses and anthropogenic reactive nitrogen creation to 52% and 64% of 2010

8 levels, respectively, in China. Fung et al. (2019) showed that the maize-soybean intercropping improves NUE by easing

9 fertilizer application and NH_3 volatilization in agricultural soils in China. Therefore, we acknowledge that the future paths of

10 agricultural NH_3 emission and nitrogen deposition may differ from what we projected as a worst-case scenario in this study,

11 but we do not expect the nature of the mechanisms and conclusions in this study to be altered significantly.

12

13 Atmospheric nitrogen deposition increases carbon uptake by terrestrial biosphere in nitrogen-limited areas, and also stimulates

14 release of NO_x, nitrous oxide (N_2O) and NH_3 from soils (Reis et al., 2009; Zaehle et al., 2011). We found that nitrogen

15 deposition increases by 20% from year 2000 to 2050 due to rising agricultural NH_3 emission, and this enhances global GPP

16 by 2.1 Pg C yr^{-1}. LAI was simulated to be higher by up to 0.3–0.4 m^2 m^{-2} in tropical grasslands and croplands, and 0.1–0.2

17 m^2 m^{-2} in midlatitude boreal and temperate forests. Canopy height increases were found in boreal and temperate forests (by

18 0.1–0.4 m), as well as in tropical grasslands and croplands (by ~0.1 m). Soil NO_x emission budget rises to 8.7 Tg N yr^{-1} with

19 year-2050 nitrogen deposition because of intensive nitrification and denitrification processes. Due to decreasing trends of

20 anthropogenic NO_x emission throughout this century (IPCC, 2013), soil NO_x is expected to play an increasingly important role

21 in global NO_x budget. Therefore, the inclusion of effects of soil NO_x emission to surface ozone is essential. These estimates

22 are based on carbon and nitrogen interactions in CLM4.5 biogeochemistry (CLM4.5-BGC), which are widely used in

23 estimating long-term trajectory of terrestrial variations (Lombardozzi et al., 2012; Val Martin et al., 2014; Sadiq et al., 2017;

24 Zhou et al., 2018). However, the internal soil nitrogen cycle, its coupling with the atmosphere and reactive nitrogen gas

25 emissions other than N_2O are not fully represented in default CLM4.5-BGC. The soil NO_x emission module that we added,

26 which allows soil NO_x to respond to nitrogen deposition from the atmosphere, partly improved the representation (Fung et al.,

27 2021), but the NH_3 emission we used was still based on inventories and scaling with future crop production and thus did not

28 respond to nitrogen deposition. We expect, however, that the secondary effect of nitrogen deposition on NH_3 should be much

29 smaller than any perturbations due to agricultural changes (Fung et al., 2021). Moreover, fully coupled bidirectional nitrogen

30 fluxes were not enabled in our model setting. Future work is needed to examine the overall downstream biogeochemical and

31 biogeophysical effects in an Earth system model with a closed nitrogen cycle where soil NO_x and NH_3 emissions to the

32 atmosphere and nitrogen deposition from the atmosphere are fully coupled dynamically.

33

34 With only the biogeochemical effects of nitrogen-induced terrestrial changes (with prescribed meteorology where

35 meteorological changes are not included), surface ozone is elevated by 1–3 ppbv in certain low-NO_x equatorial regions due to

36 increased soil NO_x emission, while LAI and canopy height only modulate surface ozone by ±0.5 and 0.2 ppbv, respectively.

37 With both the biogeochemical and biogeophysical effects under dynamic meteorology, changes in summertime surface ozone

38 are within ±2–3 ppbv. Ozone responses due to vegetation changes are much higher with dynamic meteorology than prescribed

39 meteorology, as vegetation changes shift surface energy balance, circulation patterns, moisture flow, and thus shape ozone

40 concentrations. Local meteorological variations induced by vegetation structural changes are generally more important than

41 the vegetation changes per se in terms of modulating surface ozone concentration, and appear to be as important as

42 biogeochemical soil NO_x effect. Furthermore, biogeophysical pathways related to canopy height changes have not been

43 accounted for by most previous studies of ozone-vegetation interactions, which usually only considered LAI and other

ecophysiological changes (Wang et al, 2020; Wong et al., 2018; Zhao et al., 2017; Fu et al., 2015). Global vegetation growth is altered by land use and land cover change, warming, CO_2 fertilization, nitrogen deposition and ozone damage, etc., but the associated canopy height changes have usually been ignored, rendering an incomplete representation of terrestrial effects on surface air quality predictions. Here, we found that the effects of canopy height changes on surface ozone through the biogeophysical pathways are noticeable and can be as much as the effects associated with LAI changes alone.

One limitation of this study is that we did not consider ozone damage on stomatal conductance and photosynthesis as in the study by Sadiq et al. (2017). If ozone damage on stomatal conductance is considered, higher ozone concentrations could have positive feedbacks on ozone itself via reduced dry deposition and enhanced isoprene emission. Meanwhile, ozone damage on plant productivity may also diminish the fertilization effect of nitrogen and foliar nitrogen content, which is itself vital for photosynthetic capacity (Franz and Zaehle, 2021). Therefore, if ozone damage is considered, lower LAI and canopy height are expected, compensating some of the enhanced LAI and canopy height induced by higher nitrogen deposition found in this study. These changes in LAI and canopy height could further affect ozone via various biogeochemical and biogeophysical pathways, but such a secondary feedback effect is expected to be relatively minor (Zhou et al., 2018). More work is warranted to investigate the individual and combined effects of nitrogen deposition and ozone damage on plant growth and terrestrial carbon uptake, especially in light of the possible nonlinear interactions between ozone and nitrogen in plants (e.g., Shang et al., 2021).

Overall, our study demonstrates a novel linkage between agricultural activities and ozone air quality via the modulation of vegetation and soil biogeochemistry by nitrogen deposition, and highlights the particular importance of considering meteorological changes following vegetation structural changes including those in canopy height, as well as soil NO_x changes, in studying the effects of ozone-nitrogen-vegetation interactions in the future.

Data availability

Model output data used for analysis and plotting can be made available in RData format by contacting the corresponding author (Amos P. K. Tai: amostai@cuhk.edu.hk).

Author contributions

A.P.K.T. devised the overall methodology and supervised the writing of the manuscript. X.L. conducted model simulation, analyzed results and drafted the manuscript. K.M.F. implemented soil NO_x and NH_3 emission in the model.

Competing interests

The authors declare that they have no conflict of interest.

References

Alexandratos, N. and Bruinsma, J.: World agriculture towards 2030/2050: the 2012 revision, ESA working paper No. 12-03, FAO, Rome, 2012.

Avnery, S., Mauzerall, D. L., Liu, J., and Horowitz, L. W.: Global crop yield reductions due to surface ozone exposure: 1. Year 2000 crop production losses and economic damage, Atmos. Environ., 45, 2284–2296, https://doi.org/10.1016/j.atmosenv.2010.11.045, 2011.

Baron, J. S., Barber, M., Adams, M., Agboola, J. I., Allen, E. B., Bealey, W. J., Bobbink, R., Bobrovsky, M. V., Bowman, W. D., Branquinho, C. and Bustamente, M. M.: The Effects of Atmospheric Nitrogen Deposition on Terrestrial and Freshwater Biodiversity, Springer Netherlands, Dordrecht, 465-480, http://doi.org/10.1007/978-94-007-7939-6, 2014.

Bauer, S. E., Tsigaridis, K., and Miller, R.: Significant atmospheric aerosol pollution caused by world food cultivation, Geophys. Res. Lett., 43, 5394–5400, https://doi.org/10.1002/2016GL068354, 2016.

Behera, S. N., Sharma, M., Aneja, V. P., and Balasubramanian, R.: Ammonia in the atmosphere: a review on emission sources, atmospheric chemistry and deposition on terrestrial bodies, Environ. Sci. Pollut. Res. Int., 20, 8092–8131, https://doi.org/10.1007/s11356-013-2051-9, 2013.

Bergstrom, A. K. and Jansson, M.: Atmospheric nitrogen deposition has caused nitrogen enrichment and eutrophication of lakes in the northern hemisphere, Global Change Biol., 12, 635–643, https://doi.org/10.1111/j.1365-2486.2006.01129.x, 2006.

Beusen, A. H. W., Bouwman, A. F., Heuberger, P. S. C., Van Drecht, G., and Van Der Hoek, K. W.: Bottom-up uncertainty estimates of global ammonia emissions from global agricultural production systems, Atmos. Environ., 42, 6067–6077, doi:10.1016/j.atmosenv.2008.03.044, 2008.

Bittman, S., and Mikkelsen R.: Ammonia emissions from agricultural operations: livestock, Better Crops, 93, 28–31, 2009.

Bonan, G.: Ecological Climatology, Cambridge University Press, 3rd Edn., 2016

Bonan, G. B., Lawrence, P. J., Oleson, K. W., Levis, S., Jung, M., Reichstein, M., Lawrence, D. M., and Swenson, S. C.: Improving canopy processes in the Community Land Model version 4 (CLM4) using global flux fields empirically inferred from FLUXNET data, J. Geophys. Res.-Biogeo., 116, G02014, doi:10.1029/2010jg001593, 2011.

Canfield, D. E., Glazer, A. N., and Falkowski, P. G.: The evolution and future of Earth's nitrogen cycle, Science, 330, 192-196, doi:10.1126/science.1186120, 2010.

Ciais, P., Sabine, C., Bala, G., Bopp, L., Brovkin, V., Canadell, J., Chhabra, A., DeFries, R., Galloway, J., Heimann, M., Jones, C., Quéré, C. L., Myneni, R. B., Piao, S., and Thornton, P.: Chapter 6: Carbon and Other Biogeochemical Cycles, in: IPCC, Climate Change 2013: The Physical Science Basis. Contribution of Working Group I to the Fifth Assessment Report of the Intergovernmental Panel on Climate Change, edited by: Stocker, T. F., Qin, D., Plattner, G.-K., Tignor, M., Allen, S. K., Boschung, J., Nauels, A., Xia, Y., Bex, V., and Midgley, P. M., Cambridge University Press, Cambridge, United Kingdom and New York, NY, USA, 465–570, 2013.

Ellis, R. A., Jacob, D. J., Sulprizio, M. P., Zhang, L., Holmes, C. D., Schichtel, B. A., Blett, T., Porter, E., Pardo, L. H., and Lynch, J. A.: Present and future nitrogen deposition to national parks in the United States: critical load exceedances, Atmos. Chem. Phys., 13, 9083–9095, https://doi.org/10.5194/acp13-9083-2013, 2013.

Erisman, J. W., Sutton, M. A., Galloway, J., Klimont, Z., and Winiwarter, W.: How a century of ammonia synthesis changed the world, Nat. Geosci., 1, 636–639, doi:10.1038/ngeo325, 2008.

Fenn, M. E., Allen, E. B., Weiss, S. B., Jovan, S., Geiser, L. H., Tonnesen, G. S., Johnson, R. F., Rao, L. E., Gimeno, B. S., Yuan, F., Meixner, T., and Bytnerowicz, A.: Nitrogen critical loads and management alternatives for N-impacted ecosystems in California, J. Environ. Manage., 91, 2404–2423, doi:10.1016/J.Jenvman.2010.07.034, 2010.

Fu, X., Wang, S. X., Ran, L. M., Pleim, J. E., Cooter, E., Bash, J. O., Benson, V., and Hao, J. M.: Estimating NH3 emissions from agricultural fertilizer application in China using the bi- directional CMAQ model coupled to an agro-ecosystem model, Atmos. Chem. Phys., 15, 6637–6649, doi:10.5194/acp-15-6637- 2015, 2015.

Fu, Y., and Tai A. P. K.: Impact of climate and land cover changes on tropospheric ozone air quality and public health in East Asia between 1980 and 2010, Atmos. Chem. Phys., 15, 10093–10106, doi:10.5194/acp-15-10093-2015, 2015.

Fung, K. M., Tai, A. P., Yong, T., Liu, X., and Lam, H. M. Co-benefits of intercropping as a sustainable farming method for safeguarding both food security and air quality. Environmental Research Letters, 14(4), 044011, doi.org/10.1088/1748-9326/aafc8b, 2019.

Fung, K. M., Val Martin, M., and Tai, A. P. K.: Modeling the interinfluence of fertilizer-induced NH3 emission, nitrogen deposition, and aerosol radiative effects using modified CESM2, Biogeosciences Discuss. [preprint], doi.org/10.5194/bg-2021-63, in review, 2021.

Franz, M., & Zaehle, S. Competing effects of nitrogen deposition and ozone exposure on northern hemispheric terrestrial carbon uptake and storage, 1850–2099. Biogeosciences, 18(10), 3219-3241, doi.org/10.5194/bg-18-3219-2021, 2021.

Galloway, J. N., Aber, J. D., Erisman, J. W., Seitzinger, S. P., Howarth, R. W., Cowling, E. B., and Cosby, J.: The nitrogen cascade, BioScience, 53, 341–356, doi:10.1641/0006- 3568(2003)053[0341:TNC]2.0.CO;2, 2003.

Galloway, J. N., Townsend, A. R., Erisman, J. W., Bekunda, M., Cai, Z., Freney, J. R., Martinelli, L. A., Seitzinger, S. P., and Sutton, M. A.: Transformation of the Nitrogen Cycle: Recent trends, questions, and potential solutions, Science, 320, 889–892, doi: 10.1126/science.1136674, 2008.

Geddes, J. A. and Martin, R. V.: Global deposition of total reactive nitrogen oxides from 1996 to 2014 constrained with satellite observations of NO2 columns, Atmos. Chem. Phys., 17, 10071–10091, doi.org/10.5194/acp-17-10071-2017, 2017

Gruber, N. and Galloway, J. N.: An Earth-system perspective of the global nitrogen cycle, Nature, 451, 293–296, doi:10.1038/nature06592, 2008.

1   Gu, B. J., Ge, Y., Ren, Y., Xu, B., Luo, W. D., Jiang, H., Gu, B. H., and Chang, J.: Atmospheric reactive nitrogen in China:

2   Sources, recent trends, and damage costs, Environ. Sci. Technol., 46, 9240–9247, doi:10.1021/es301446g, 2012.

3

4   Gu, B., Ju. X., Chang. J., Ge, Y., and Vitousek P. M.: Integrated reactive nitrogen budgets and future trends in China, P. Natl.

5   Acad. Sci. USA, 112(28), 8792–8797, doi.org/10.1073/pnas.1510211112, 2015.

6

7   Gu, B. J., Sutton, M. A., Chang, S. X., Ge, Y., and Jie, C.: Agricultural ammonia emissions contribute to China's urban air

8   pollution, Front. Ecol. Environ., 12, 265–266, doi:10.1890/14.WB.007, 2015.

9

10   Guenther, A. B., Jiang, X., Heald, C. L., Sakulyanontvittaya, T., Duhl, T., Emmons, L. K., and Wang, X.: The Model of

11   Emissions of Gases and Aerosols from Nature version 2.1 (MEGAN2.1): an extended and updated framework for modeling

12   biogenic emissions, Geosci. Model Dev., 5, 1471–1492, doi:10.5194/gmd-5-1471-2012, 2012.

13

14   He, L., Chen, J. M., Croft, H., Gonsamo, A., Luo, X., Liu, J., Zheng, T., Liu, R., Liu, Y.: Nitrogen availability dampens the

15   positive impacts of CO2 fertilization on terrestrial ecosystem carbon and water cycles. Geophys. Res. Lett., 44, 11590–11600,

16   https://doi.org/10.1002/ 2017GL075981, 2017.

17

18   Heald, C. L., and Geddes, J. A.: The impact of historical land use change from 1850 to 2000 on secondary particulate matter

19   and ozone, Atmos. Chem. Phys., 16, 14997–15010, doi: 10.5194/acp-16-14997-2016, 2016.

20

21   Heimann, M. and Reichstein, M.: Terrestrial ecosystem carbon dynamics and climate feedbacks, Nature, 451, 289–292,

22   doi.org/10.1038/nature06591, 2008.

23

24   Huang, X., Song, Y., Li, M., Li, J., Huo, Q., Cai, X., Zhu, T., Hu, M., and Zhang, H.: A high-resolution ammonia emission

25   inventory in China, Global Biogeochem. Cy., 26, GB1030, doi:10.1029/2011GB004161, 2012.

26

27   Jerrett, M., Burnett, R. T., Pope, A. C., Ito, K., Thurston, G., Krewski, D., Shi, Y., Calle, E., and Thun, M.: Long-Term Ozone

28   Exposure and Mortality, New England Journal of Medicine, 360, 1085–1095, doi:10.1056/NEJMoa0803894, 2009.

29

30   Kanakidou, M., Myriokefalitakis, S., Daskalakis, N., Fanourgakis, G., Nenes, A., Baker, A. R., Tsigaridis, K., and

31   Mihalopoulos, N.: Past, present and future atmospheric nitrogen deposition, J. Atmos. Sci., 73, 2039–2047,

32   doi.org/10.1175/JAS-D-15-0278.1, 2016.

33

34   Kang, Y., Liu, M. , Song, Y., Huang, X. , Yao, H., Cai, X., Zhang, H., Kang, L., Liu, X., Yan, X., He, H., Zhang, Q., Shao,

35   M., and Zhu, T.: High-resolution ammonia emissions inventories in China from 1980 to 2012, Atmos. Chem. Phys., 16, 2043–

36   2058, doi.org/10.5194/acp-16-2043-2016, 2016.

37

38   Lamarque, J.-F., Kyle, G. P., Meinshausen, M., Riahi, K., Smith, S. J., Vuuren, D. P., Conley, A. J., and Vitt, F.: Global and

39   regional evolution of short-lived radiatively-active gases and aerosols in the Representative Concentration Pathways, Clim.

40   Change, 109, 191–212, doi:10.1007/s10584-011-0155-0, 2011.

41

Lamarque, J.-F., Emmons, L. K., Hess, P. G., Kinnison, D. E., Tilmes, S., Vitt, F., Heald, C. L., Holland, E. A., Lauritzen, P. H., Neu, J., Orlando, J. J., Rasch, P. J., and Tyndall, G. K.: CAM-chem: description and evaluation of interactive atmospheric chemistry in the Community Earth System Model, Geosci. Model Dev., 5, 369-411, doi:10.5194/gmd-5-369-2012, 2012.

Lamarque, J.-F., Shindell, D. T., Josse, B., Young, P. J., Cionni, I., Eyring, V., Bergmann, D., Cameron-Smith, P., Collins, W. J., Doherty, R., Dalsoren, S., Faluvegi, G., Folberth, G., Ghan, S. J., Horowitz, L. W., Lee, Y. H., MacKenzie, I. A., Nagashima, T., Naik, V., Plummer, D., Righi, M., Rumbold, S. T., Schulz, M., Skeie, R. B., Stevenson, D. S., Strode, S., Sudo, K., Szopa, S., Voulgarakis, A., and Zeng, G.: The Atmospheric Chemistry and Climate Model Intercomparison Project (ACCMIP): overview and description of models, simulations and climate diagnostics, Geosci. Model Dev., 6, 179–206, doi:10.5194/gmd-6-179-2013, 2013.

Lawrence, D. M., Oleson, K. W., Flanner, M. G., Thornton, P. E., Swenson, S. C., Lawrence, P. J., Zeng, X. B., Yang, Z. L., Levis, S., Sakaguchi, K., Bonan, G. B., and Slater, A. G.: Parameterization Improvements and Functional and Structural Advances in Version 4 of the Community Land Model, J. Adv. Model Earth Sy., 3, M03001, doi:10.1029/2011MS000045, 2011.

LeBauer, D. S., and Treseder, K. K.: Nitrogen limitation of net primary productivity in terrestrial ecosystems is globally distributed, Ecology, 89(2), 371–379, doi.org/10.1890/06-2057.1, 2008.

Li, Y., Schichtel, B. A., Walker, J. T., Schwede, D. B., Chen, X., Lehmann, C. M., Puchalski, M. A., Gay, D. A., and Collett, J. L.: Increasing importance of deposition of reduced nitrogen in the United States, P. Natl. Acad. Sci. USA, 113, 5874-5879, doi.org/10.1073/pnas.1525736113, 2016.

Liu, M. L. and Tian, H. Q.: China's land cover and land use change from 1700 to 2005: Estimations from high-resolution satellite data and historical archives, Global Biogeochem. Cy., 24, GB3003, doi:10.1029/2009gb003687, 2010.

Liu, J., Ma, K., Ciais, P., and Polasky, S.: Reducing human nitrogen use for food production. Sci. Rep. 6, 30104; doi: 10.1038/srep30104, 2016.

Lombardozzi, D., Levis, S., Bonan, G., and Sparks, J. P.: Predicting photosynthesis and transpiration responses to ozone: decoupling modeled photosynthesis and stomatal conductance, Biogeosciences, 9, 3113–3130, doi:10.5194/bg-9-3113-2012, 2012.

Lu, X., Mao, Q., Gilliam, F. S., Luo, Y., and Mo, J.: Nitrogen deposition contributes to soil acidification in tropical ecosystems, Glob. Change Biol., 20, 3790–3801, doi.org/10.1111/gcb.12665, 2014.

Mueller, N. D., Lassaletta, L., Runck, B. C., Billen, G., Garnier, J., and Gerber, J. S.: Declining spatial efficiency of global cropland nitrogen allocation, Global Biogeochemical Cycles, 31, 245–257, doi.org/10.1002/2016GB005515, 2017.

Oleson, K. W., Lawrence, D. M., Bonan, G. B., Drewniak, B., Huang, M., Koven, C. D., Levis, S., Li, F., Riley, W. J., Subin, Z. M., Swenson, S. C., Thornton, P. E., Bozbiyik, A., Fisher, R., Heald, C. L., Kluzek, E., Lamarque, J.-F., Lawrence, P. J., Leung, L. R., Lipscomb, W., Muszala, S., Ricciuto, D. M., Sacks, W., Sun, Y., Tang, J., and Yang, Z.-L.: Technical Description

1　of version 4.5 of the Community Land Model (CLM). Ncar Technical Note NCAR/TN-503+STR, National Center for
2　Atmospheric Research, 422, doi.org/10.5065/D6RR1W7M, 2013.

3

4　Paulot, F., Jacob, D. J., and Henze, D. K.: Sources and processes contributing to nitrogen deposition in biodiversity hotspots
5　worldwide, Environ. Sci. Technol., 47, 3226–3233, doi:10.1021/es3027727, 2013.

6

7　Paulot, F., Jacob, D. J., Pinder, R. W., Bash, J. O., Travis, K., and Henze, D. K.: Ammonia emissions in the United States,
8　European Union, and China derived by high-resolution inversion of ammonium wet deposition data: interpretation with a new
9　agricultural emissions inventory (MASAGE_NH3), J. Geophys. Res.-Atmos., 119, 4343-4364,
10　doi.org/10.1002/2013JD021130, 2014.

11

12　Pozzer, A., Tsimpidi, A. P., Karydis, V. A., de Meij, A. and Lelieveld, J.: Impact of agricultural emission reductions on fine-
13　particulate matter and public health, Atmos. Chem. Phys., 17(20), 12813–12826, doi.org/10.5194/acp-17-12813-2017, 2017.

14

15　Rayner, N. A., Parker, D. E., Horton, E. B., Folland, C. K., Alexander, L. V., Rowell, D. P., Kent, E. C., and Kaplan, A.:
16　Global analyses of sea surface temperature, sea ice, and night marine air temperature since the late nineteenth century, J.
17　Geophys. Res.- Atmos., 108, D002670, doi.org/10.1029/2002JD002670, 2003.

18

19　Reay, D. S., Dentener, F., Smit, P., Grace, J., and Feely, R. A.: Global nitrogen deposition and carbon sinks, Nature Geosci.,
20　1, 430–437, doi.org/10.1038/ngeo23010.1038/ngeo230, 2008.

21

22　Reis, S., Pinder, R. W., Zhang, M., Lijie, G., and Sutton, M. A.: Reactive nitrogen in atmospheric emission inventories, Atmos.
23　Chem. Phys., 9, 7657–7677, doi:10.5194/acp-9-7657-2009, 2009.

24

25　Rodríguez, L. and Macías, F.: Eutrophication trends in forest soils in Galicia (NW Spain) caused by the atmospheric deposition
26　of nitrogen compounds, Chemosphere, 63, 1598–1609, doi.org/10.1016/j.chemosphere.2005.08.072, 2006.

27

28　Sadiq, M., Tai, A. P. K., Lombardozzi, D., and Val Martin, M.: Effects of ozone-vegetation coupling on surface ozone air
29　quality via biogeochemical and meteorological feedbacks, Atmos. Chem. Phys., 17, 3055–3066, doi.org/10.5194/acp-17-
30　3055-2017, 2017.

31

32　Shang, B., Xu, Y., Peng, J., Agathokleous, E., & Feng, Z. High nitrogen addition decreases the ozone flux by reducing the
33　maximum stomatal conductance in poplar saplings. Environmental Pollution, 272, 115979,
34　doi.org/10.1016/j.envpol.2020.115979, 2021.

35

36　Sheppard, L. J., Leith, I. D., Mizunama, T., Cape, J. N., Crossley, A., Leeson, S., Sutton, M. A., van Dijk, N., and Fowler, D.:
37　Dry deposition of ammonia gas drives species change faster than wet deposition of ammonium ions: evidence from a longterm
38　field manipulation, Glob. Change. Biol., 17, 3589–3607, doi:10.1111/j.1365-2486.2011.02478.x, 2011.

39

40　Sokolov, A. P., Kicklighter, D. W., Melillo, J. M., Felzer, B., Schlosser, C. A., and Cronin, T. W.: Consequences of considering
41　carbon/nitrogen interactions on the feedbacks between climate and the terrestrial carbon cycle, J. Climate, 21, 3776–3796,
42　doi.org/10.1175/2008JCLI2038.1, 2008.

43

Streets, D. G., Bond, T. C., Carmichael, G. R., Fernandes, S. D., Fu, Q., He, D., Klimont, Z., Nelson, S. M., Tsai, N. Y., Wang, M. Q., Woo, J.-H., and Yarber, K. F.: An inventory of gaseous and primary aerosol emissions in Asia in the year 2000, J. Geophys. Res., 108, 8809, doi:10.1029/2002JD003093, 2003.

Sutton, M. A., Reis, S., Riddick, S. N., Dragosits, U., Nemitz, E., Theobald, M. R., Tang, Y. S., Braban, C. F., Vieno, M., Dore, A. J., Mitchell, R. F., Wanless, S, Daunt, F., Fowler, D., Blackall, T. D., Milford, C., Flechard, C. R., Loubet, B., Massad, R., Cellier, P., Personne, E., Coheur, P. F., Clarisse, L., Van Damme, M., Ngadi, Y., Clerbaux, C., Skjøth, C. A., Geels, C., Hertel, O., Wichink Kruit, R. J., Pinder, R. W., Bash, J. O., Walker, J. T., Simpson, D., Horváth, L., Misselbrook, T. H., Bleeker, A., Dentener, F., and de Vries, W.: Towards a climate-dependent paradigm of ammonia emission and deposition, Philos. Trans. R. Soc. B. Biol. Sci., 368, 20130166, doi:10.1098/rstb.2013.0166, 2013.

Tai, A.P., Martin, M.V. and Heald, C.L.,: Threat to future global food security from climate change and ozone air pollution. Nature Climate Change, 4(9), 817–821, doi.org/10.1038/nclimate2317, 2014.

Tai, A.P. and Martin, M.V.: Impacts of ozone air pollution and temperature extremes on crop yields: Spatial variability, adaptation and implications for future food security. Atmospheric Environment, 169, 11–21, doi.org/10.1016/j.atmosenv.2017.09.002, 2017.

Tan, J., Fu, J. S., Dentener, F., Sun, J., Emmons, L., Tilmes, S., Flemming, J., Takemura, T., Bian, H., Zhu, Q., Yang, C., Keating, T.: Multi-model study of HTAP II on sulfur and nitrogen deposition, Atmos. Chem. Phys., 18, 6847-6866, doi.org/10.5194/acp-18-6847-2018, 2018.

Templer, P. H., Pinder, R. W., and Goodale, C. L.: Effects of nitrogen deposition on greenhouse-gas fluxes for forests and grasslands of North America, Front Ecol. Environ., 10, 547-553, doi:10.1890/120055, 2012.

Tian, H., Banger, K., Bo, T., and Dadhwal, V. K.: History of land use in India during 1880–2010: Large-scale land transformations reconstructed from satellite data and historical archives, Global and Planetary Change, 121, 78–88. https://doi.org/10.1016/j.gloplacha.2014.07.005,2014

Tilman, D., Cassman, K. G., Matson, P. A., Naylor, R., and Polasky, S.: Agricultural sustainability and intensive production practices, Nature, 418, 671–677, doi.org/10.1038/nature01014, 2002.

Thornton, P. E., Lamarque, J.-F., Rosenbloom, N. A., and Mahowald, N. M.: Influence of carbon-nitrogen cycle coupling on land model response to CO2 fertilization and climate variability, Global Biogeochem. Cy., 21, GB4018, doi:10.1029/2006GB002868, 2007.

Thornton, P. E., Doney, S. C., Lindsay, K., Moore, J. K., Mahowald, N., Randerson, J. T., Fung, I., Lamarque, J.-F., Feddema, J. J., and Lee, Y.-H.: Carbon-nitrogen interactions regulate climate-carbon cycle feedbacks: results from an atmosphereocean general circulation model, Biogeosciences, 6, 2099–2120, doi:10.5194/bg-6-2099-2009, 2009.

van Vuuren, D. P., Edmonds, J., Kainuma, M., Riahi, K., Thomson, A., Hibbard, K., Hurtt, G. C., Kram, T., Krey, V., Lamarque, J. F., Masui, T., Meinshausen, M., Nakicenovic, N., Smith, S. J., and Rose, S. K.: The representative concentration pathways: an overview, Climatic Change, 109, 5–31, doi.org/10.1007/s10584-011-0148-z, 2011.

Val Martin, M., Heald, C. L., and Arnold, S. R.: Coupling dry deposition to vegetation phenology in the Community Earth System Model: Implications for the simulation of surface O3, Geophys. Res. Lett., 41, 2988-2996, doi:10.1002/2014GL059651, 2014.

Vitousek, P. M., Hättenschwiler, S., Olander, L., and Allison, S.: Nitrogen and Nature, A Journal of the Human Environment, 31(2), 97–102, doi.org/10.1579/0044-7447-31.2.97, 2002.

Wang, L., Tai, A.P., Tam, C.Y., Sadiq, M., Wang, P. and Cheung, K.K.,: Impacts of future land use and land cover change on mid-21st-century surface ozone air quality: distinguishing between the biogeophysical and biogeochemical effects, Atmos. Chem. Phys., 20, 11349–11369, doi.org/10.5194/acp-20-11349-2020, 2020.

Wong, A. Y. H., Tai, A. P. K., and Ip, Y. Y.: Attribution and statistical parameterization of the sensitivity of surface ozone to changes in leaf area index based on a chemical transport model, J. Geophys. Res.-Atmos., 123, 1883–1898, doi.org/10.1002/2017JD027311, 2018.

Xu, R. T., Pan, S. F., Chen, J., Chen, G. S., Yang, J., Dangal, S. R. S., Shepard, J. P., and Tian, H. Q.: Half-century ammonia emissions from agricultural systems in southern Asia: Magnitude, spatiotemporal patterns and implications for human health, GeoHealth, 2, 40–53, doi.org/ 10.1002/2017GH000098, 2018.

Xu, W., Luo, X. S., Pan, Y. P., Zhang, L., Tang, A. H., Shen, J. L., Zhang, Y., Li, K. H., Wu, Q. H., Yang, D. W., Zhang, Y. Y., Xue, J., Li, W. Q., Li, Q. Q., Tang, L., Lu, S. H., Liang, T., Tong, Y. A., Liu, P., Zhang, Q., Xiong, Z. Q., Shi, X. J., Wu, L. H., Shi, W. Q., Tian, K., Zhong, X. H., Shi, K., Tang, Q. Y., Zhang, L. J., Huang, J. L., He, C. E., Kuang, F. H., Zhu, B., Liu, H., Jin, X., Xin, Y. J., Shi, X. K., Du, E. Z., Dore, A. J., Tang, S., Collett Jr., J. L., Goulding, K., Sun, Y. X., Ren, J., Zhang, F. S., and Liu, X. J.: Quantifying atmospheric nitrogen deposition through a nationwide monitoring network across China, Atmos. Chem. Phys., 15, 12345–12360, doi:10.5194/acp-15-12345-2015, 2015.

Zaehle, S., Friedlingstein, P., and Friend, A. D. Terrestrial nitrogen feedbacks may accelerate future climate change, Geophys. Res. Lett., 37, L01401, doi.org/10.1029/2009GL04134510.1029/2009GL041345, 2010.

Zaehle, S., Ciais, P., Friend, A. D., and Prieur, V.: Carbon benefits of anthropogenic reactive nitrogen offset by nitrous oxide emissions, Nat. Geosci., 4, 601–605, doi:10.1038/ngeo1207, 2011.

Zhao, Y., Zhang, L., Tai, A. P. K., Chen, Y., and Pan, Y.: Responses of surface ozone air quality to anthropogenic nitrogen deposition in the Northern Hemisphere, Atmos. Chem. Phys., 17, 9781–9796, doi.org/10.5194/acp-17-9781-2017, 2017.

Zhang, L., Chen, Y., Zhao, Y., Henze, D. K., Zhu, L., Song, Y., Paulot, F., Liu, X., Pan, Y., Lin, Y., and Huang, B.: Agricultural ammonia emissions in China: reconciling bottom-up and top-down estimates, Atmos. Chem. and Phys., 18, 339–355, https://doi.org/10.5194/acp-18-339-2018, 2018.

Zhang, X., Davidson, E. A., Mauzerall, D. L., Searchinger, T. D., Dumas, P., and Shen, Y.: Managing nitrogen for sustainable development, Nature, 528, 51–59, doi.org/10.1038/nature15743, 2015.

Zhang, X.: Biogeochemistry: A plan for efficient use of nitrogen fertilizers, Nature, 543, 322–323, doi.org/10.1038/543322a, 2017.

Zhang, X., Wu, Y., Liu, X., Reis, S., Jin, J., Dragosits, U., Van Damme, M., Clarisse, L., Whitburn, S., Coheur, P. F., and Gu, B.: Ammonia emissions may be substantially underestimated in China, Environ. Sci. Technol., 51(21), 12089–12096, doi.org/10.1021/acs.est.7b02171, 2017

Zhou, S. S., Tai, A. P. K., Sun, S., Sadiq, M., Heald, C. L., and Geddes, J. A.: Coupling between surface ozone and leaf area index in a chemical transport model: strength of feedback and implications for ozone air quality and vegetation health, Atmos. Chem. Phys., 18, 14133–14148, doi.org/10.5194/acp-18-14133-2018, 2018.

Zhu, L., Henze, D., Bash, J., Jeong, G.-R., Cady-Pereira, K., Shephard, M., Luo, M., Paulot, F., and Capps, S.: Global evaluation of ammonia bidirectional exchange and livestock diurnal variation schemes, Atmos. Chem. Phys., 15, 12823–12843, doi:10.5194/acp-15-12823-2015, 2015.